Extractives Extend the Applicability of Multistep Kinetic Scheme of Biomass Pyrolysis

Paulo Eduardo Amaral Debiagi, Chiara Pecchi, Giancarlo Gentile, Alessio Frassoldati, Alberto Cuoci, Tiziano Faravelli, and Eliseo Ranzi*

Dipartimento di Chimica Materiali ed Ingegneria Chimica "Giulio Natta", Politecnico di Milano, Piazza Leonardo da Vinci 32, Milan, Italy

Received: July 31, 2015
Revised: September 10, 2015
Published: September 15, 2015

1. INTRODUCTION

Exponential population growth, increasing energy demand, and climate changes worldwide, caused mainly by greenhouse effect, are raising the real interest in exploitation of renewable sources of energy. Because of their almost negligible effect on atmospheric CO_2 concentrations and their more uniform distribution than fossil sources, biomasses are interesting options to answer the energy demand. Biomass comprises a broad range of different types of biomaterials, such as wood, forest and agricultural residues, waste from wood and food industry, algae, energy grasses, straw, bagasse, sewage sludge, etc. The use of different types of biomass results in different challenges and solutions for transportation, storage, and feeding, and finally for converting biomasses into more useful chemicals or substitutes for fossil fuels.[1,2] Interesting and widely available biomasses sources are wood and agricultural residues, which are usually solid, spread through the territory, generally with a high content of oxygen and moisture, reducing the heating value and increasing the transportation costs. Thus, biomass pretreatments are usually required for successive thermochemical conversion processes of biomasses.

Many researchers are directing efforts on mathematical modeling, creating tools for designing and simulating reactors and for analyzing their performances, pollutant emissions, products formation, and helping the determination of optimal operating parameters for large-scale reactors.

The kinetic modeling of thermochemical conversion of biomasses, such as pyrolysis, gasification, and combustion, is a very complex multicomponent, multiphase, and multiscale problem. The strong interactions between chemical kinetics and heat- and mass-transfer processes involved in the thermal degradation of biomasses makes the mathematical modeling difficult.[3] These models must focus on four different facets of the overall problem and require at least the following features:

- characterization of the biomass;
- solid phase kinetic scheme of the pyrolysis or devolatilization process;
- gas−solid kinetic scheme of char gasification and combustion; and
- gas phase kinetic scheme of the secondary reactions of gas and tar species.

As already mentioned, pyrolysis is one of the most important methods to convert biomass to biofuel or pyrolysis oil, which is not only a liquid energy carrier, but also a possible general source of chemicals. Moreover, pyrolysis is also the first step in gasification and combustion processes. Therefore, the pyrolysis products have attracted great analytical interest. Gas chromatography coupled with flame ionization detection (GC-FID) and two-dimensional gas chromatography coupled with time-of-flight mass spectrometry (GC×GC_TOFMS) techniques are widely used. The GC-FID allows quantifying the composition, while the GC×GC_TOFMS is used for the qualitative analysis of the biofuel. In this way, more than several hundred compounds were detected and identified, thus describing ∼80% of the pyrolysis oils.[4−6] In a parallel way, the biomass pyrolysis has been also studied with tunable synchrotron vacuum ultraviolet photoionization mass spec-

trometry (SVUV-PIMS), which performs very well in product analyses. The application of SVUV-PIMS in biomass pyrolysis allows one to describe very useful time-dependent data to better understand the kinetic mechanisms underlying biomass pyrolysis.[7]

All these analytical efforts assist in a better understanding of the effect of pyrolysis conditions and biomass type. Thus, since biomasses are complex mixtures of a huge number of different compounds, the first necessary step is an efficient characterization of the biomass composition, in terms of a limited number of reference species. Often, characterization methods simply refer to cellulose, hemicellulose, and lignin compo-nents.[8−12]

The main goal of this work is to extend the validity range of the previous biomass characterization method by analyzing and including extractive species as new reference components, enlarging, in this way, the applicability of the proposed approach.[10] Therefore, the paper is organized in the following way. Section 2 discusses the biomass composition, emphasizing the attention toward the presence and importance of extractive components. Sections 3 and 4 illustrate how the new reference species allow one to extend the applicability of biomass characterization method. Section 5 discusses the new and upgraded multistep kinetic model of biomass pyrolysis. Finally, Section 6 shows some examples of comparisons between experimental data and model predictions. Section 7 provides a conclusion and summarizes the research.

2. BIOMASS ANALYSIS AND COMPOSITION

Ligno-cellulosic biomasses are mainly composed of macromolecular substances, cellulose, hemicellulose, and lignin, together with smaller amounts of organic extractives and inorganic species that form the ashes. Biomass has a porous structure where cellulose represents an important structural element surrounded by other substances that act as matrix (hemicellulose) and encrusting (lignin) materials. Moisture is also present in biomass and can be found as hygroscopic water (mainly hydrogen bonded to the hydroxyl groups of cellulose and hemicellulose), capillary water (in liquid form in the lumens of biomass), and water vapor found in the gas phase.[13] Biomass offers important advantages as a combustion feed-stock, because of the high volatility of the fuel and the high reactivity of both the fuel and the resulting char. In comparison with coal, biomass contains much less carbon, more oxygen, higher moisture content, and has a lower density and a lower heating value. The usual methods of biomass analysis are given in Table 1,[14] while Table 2 reports a sample of typical biomass compositions.[15]

Biomasses are primarily composed of elemental C, H, and O, with a smaller amount of N, and traces of S and Cl. C and H give a positive contribution, while O reduces the heating value. Several correlations between the heating value and C, H and N are proposed in the literature.[14]

The standard methods used for the ultimate elemental analysis are well-known. However, particular attention must be paid to the moisture present in the sample. The possible presence of residual water on the dried biomass sample can result in the overestimation of hydrogen and oxygen content. As already discussed elsewhere,[16] the ultimate analysis requires expensive equipment and trained analysts, while the proximate analysis is simpler and only requires standard laboratory equipment. For this reason, a few correlations for calculating the elemental composition based on proximate analysis of biomass are available in the literature.[17]

Table 1. Methods of Biomass Fuel Analyses[a]

property	analytical method(s)
heating value	ASTM D2015, E871
particle size distribution	ASTM E828
Proximate Composition	
moisture	ASTM E871
ash	ASTM D1102 (873 K), ASTM E830 (848 K)
volatile matter	ASTM E 872, ASTM E897
fixed carbon	by difference
Ultimate Elemental Analysis	
carbon, hydrogen	ASTM E777
nitrogen	ASTM E778
sulfur	ASTM E775
chlorine	ASTM E776
oxygen	by difference
elemental ash	ASTM D3682, ASTM D2795, ASTM D4278, AOAC 14.7

[a]After Demirbas.[14]

A more complete biomass analysis would require measuring structural carbohydrates (glucose, xylose, galactose, arabinose, and mannose), lignin, extractable materials, protein, and ash. Compared to elemental analysis, these analytical methods are more complex and involve thermal, chemical, and/or enzymatic separations, which could also give rise to some degradation of the original biomass. Despite several research efforts in this direction,[18] this information is not frequently available. Data reporting both elementary and biochemical or structural compositions for the same biomass sample are not easily available. This lack of information creates difficulties to characterize biomasses for modeling purposes.

Cellulose, hemicellulose, and lignins are the major components usually constituting the largest portion of the biomass.

Cellulose is a long-chain polymer built by monomeric units of a six-carbon sugar, glucose, bonded through 1,4-β-glycosidic bonds. The chains are kept together by hydrogen bonds, which confer to the polymer an almost fully crystalline structure with few amorphous zones. It is the most present structural component in biomasses, ranging from 20% to 60% of the total mass (dry).

Hemicellulose is a second structural polymer; it is a mixture of sugars (hexoses and pentoses), mainly xylose, mannose, galactose, and arabinose. Different from cellulose, it has a shorter chain and a much more amorphous structure, because of its irregular composition and the branches present on the chain. It is present in biomasses in amounts ranging from 10% to 40% (dry), rarely in quantities greater than cellulose. It is also common to refer to the combination of cellulose and hemicellulose as "holocellulose".

Lignin is a racemic polymer composed by monomeric units of aromatic alcohols (coniferyl, sinapyl, and *p*-coumaryl alcohol), whose composition changes widely inside the entire range of biomasses, making its characterization a hard task to accomplish. It is present in biomasses in amounts ranging from 15% to 45%.

Table 2. Typical Compositions for a Range of Biomass Types[a]

	Proximate Analysis				Ultimate Analysis					
biomass	moisture	volatile matter, VM	fixed carbon, FC	ash	C	H	O	N	S	Cl
wood pine chips	4.00	81.30	14.60	0.10	52.00	6.20	41.59	0.12	0.08	0.01
willow, SRC	6.96	75.70	16.31	1.03	51.62	5.54	42.42	0.38	0.03	0.01
Miscanthus giganteus	14.20	70.40	14.10	1.30	49.10	6.40	43.98	0.26	0.13	0.13
switchgrass	7.17	73.05	15.16	4.62	49.40	5.70	44.25	0.45	0.10	0.10
wheat straw	7.78	68.83	17.09	6.30	49.23	5.78	43.99	0.64	0.10	0.26
rice husks	9.40	74.00	13.20	12.80	42.30	6.10	50.56	1.10	0.10	0.04
palm PKE	7.60	72.12	16.18	4.10	51.12	7.37	38.21	2.80	0.30	0.20
sugar cane bagasse	10.40	76.70	14.70	2.20	49.90	6.00	43.15	0.40	0.04	0.51
olive residue	6.40	65.13	19.27	9.20	54.42	6.82	37.29	1.40	0.05	0.04
cow dung	13.90	60.50	11.90	13.70	54.00	6.40	36.70	0.83	0.03	1.00
lignin	9.00	73.50	1.50	16.00	72.00	6.60	21.34	0.00	0.00	0.00

[a]After Williams et al.[15]

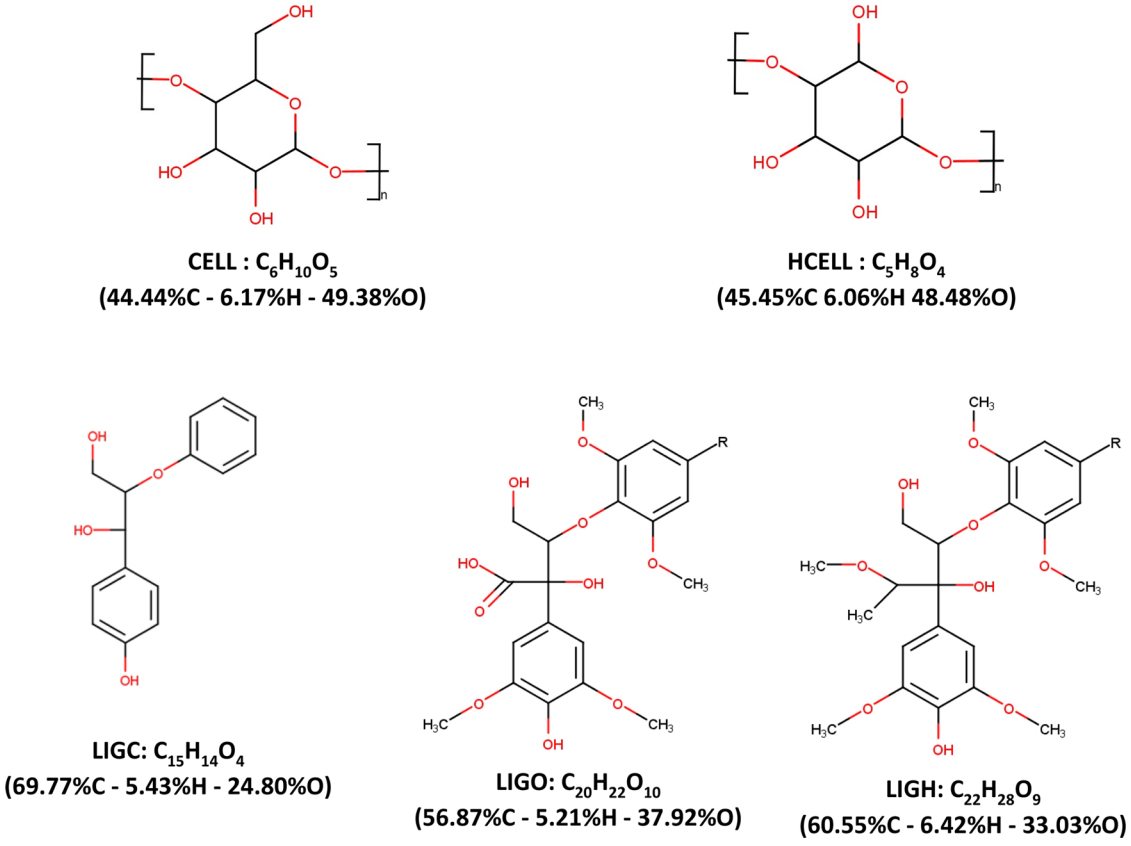

Figure 1. Reference species representing cellulose, hemicellulose, and lignins.

3. REFERENCE COMPONENTS AND CHARACTERIZATION METHOD

A very large set of more than 600 biomass samples have been collected from the databases available in the literature.[19−22] These data, in terms of their elemental and structural analysis have been organized and merged into a single database reported in the Supporting Information. The structural analysis, in terms of cellulose, hemicellulose, and lignin, is only available in <20% of the overall set of the biomass samples.

It is the usual practice to characterize the biomass in terms of the reference components: cellulose, hemicellulose, and lignin.[8−12] In particular, the approach previously proposed[10] and applied assumes the glucose monomer (with the subtraction of H_2O from the intramonomeric bonds) as the reference component (CELL) representing the cellulose polymer, $(C_6H_{10}O_5)_n$. Similarly, the xylose monomer, $(C_5H_8O_4)_n$ (again with the subtraction of H_2O from the intramonomeric bonds) is the reference component representing hemicellulose (HCELL). Because of its irregular structure, lignin can be characterized with three reference components: LIGC, LIGH, and LIGO (richer in C, H, and O, respectively). This allowed the characterization of a variety of different lignins found in angiosperm and gymnosperm biomasses.[23] Biomass pyrolysis products are assumed to be the linear combination of the pyrolysis products of the reference components. When no direct information is available on the cellulose, hemicellulose and lignin contents, the method proposed in previous papers

characterizes the biomass feedstock on the basis of its elemental H/C/O composition.[10,24]

Figure 1 shows the structure of the reference species: cellulose, hemicellulose, and the three different types of lignins. These reference species are reported in the H/C diagram in Figure 2, together with three reference mixtures (RM-1, RM-2,

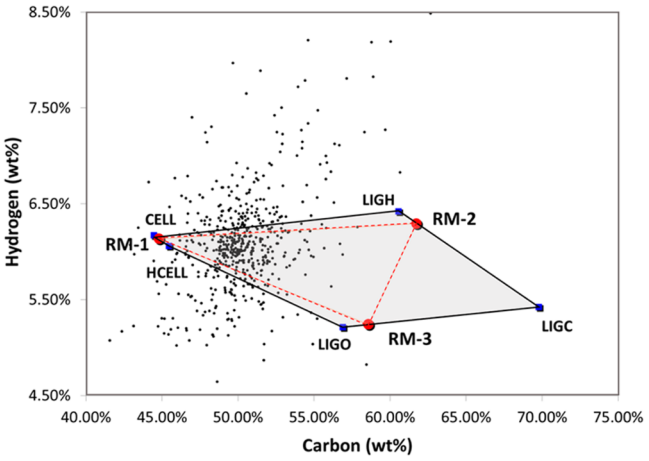

Figure 2. Biomass characterization. H% vs C% plot of biomass samples, along with their reference species (daf basis).

and RM-3), defined by three splitting parameters (α, β, and γ). α defines the molar ratio of 60% cellulose and 40% hemicellulose contained in RM1. β and γ define the two mixtures RM-2 and RM-3 of the different lignins (80% LIG-O and 20% LIG-C, and 80% LIG-H and 20% LIG-C, respectively). These parameters are the degree of freedom of this characterization procedure, which allow one to reduce the five reference species into three mixtures. Any feedstock is then considered as a linear combination of those three reference mixtures, in order to respect the given H/C/O elemental composition. The cellulose/hemicellulose ratio is assumed to be equal 1.5 as a default and most probable ratio. Of course, it can be modified when different experimental data are available. Therefore, the default splitting parameter α (cellulose/holocellulose ratio) becomes 0.6. Similarly, β and γ (or the two-lignin mixtures) can be modified to allow the characterization of biomass samples with higher, or lower, hydrogen contents.

As an example, the almond shell[22] with elemental composition H/C/O = 0.060/0.500/0.440 on a dry and ash-free (daf) basis is characterized by the following mass composition:

CELL = 0.4314 HCELL = 0.2344

LIGH = 0.1529 LIGO = 0.1376 LIGC = 0.0437

The values reported above are obtained by using the default splitting parameters: $\alpha/\beta/\gamma$ = 0.6/0.8/0.8.

With the same splitting parameters, the softwood bark[25] with H/C/O = 0.06/0.534/0.406 is characterized by the following mass composition:

CELL = 0.2936 HCELL = 0.1595

LIGH = 0.2934 LIGO = 0.1822 LIGC = 0.0713

A multistep kinetic scheme for the pyrolysis of cellulose, hemicellulose, and the three lignins describes the formation of volatiles and residual char. It involves 20 real and/or equivalent and lumped species.[10] The product composition provided by this kinetic scheme was already validated with several experimental data obtained from pyrolysis of small and thick biomass particles.[24] The limits of this characterization method and kinetic scheme is that extractives and catalytic effects of ashes are not considered. Further details on this approach were already reported in the previously referred papers.

The marks shown in Figure 2 represent the biomass data reported in the Supporting Information. It is evident from this figure that several biomass samples fall within the triangles bounded by the reference components (RM), here obtained with the default splitting parameters. Samples which fall within the shadow area can be described as a linear combination of the three RMs (which means as a combination of the five reference components). In contrast, there are several biomass samples whose compositions fall outside this area and thus cannot be represented by a feasible combination of the reference components. These biomasses are generally rich in extractives, as reported in Table 3 for a few samples.

Table 3. Biomass Samples Rich in Extractives

sample	ref	C	H	O	extractives	solvent(s)
hybrid poplar	19	50.92	5.65	43.43	6.89	ethanol
switchgrass	19	50.19	5.64	44.17	16.99	ethanol
olive husks	26	54.89	6.96	38.15	9.40	alcohol, benzene (1/1, v/v)
pinewood	26	49.00	6.40	44.60	14.90	ethanol, water, hexane

4. EXTRACTIVES AND EXTENDED BIOMASS CHARACTERIZATION METHOD

Previous considerations partially highlight the importance of extractive species. Wood plants are usually classified as angiosperm or hardwood and gymnosperm or softwood. Angiosperms are the wood plants that produce flowers and fruits. Gymnosperms are the plants that produce naked seeds. Usually, cellulose, hemicellulose, and lignin account for more than 90% of the entire biomass; thus, extractives are usually <10%. Thousands of different extractives can be identified and they present a great variety of composition, structure, and biological functions, also depending on the different seasons. They are also distributed in different ways among the organs of the plant, being more abundant in leaves and barks. Gymnosperms generally are richer in extractives, which can even reach more than 20% in bark samples. Because of the large variety of extractive species, it is necessary to drastically simplify the complexity of the overall system. Therefore, the objective is to identify the most common and widely present group of extractive molecules and to define a couple of lumped species that are reasonably representative of these species. Water solubility is a simple and useful way to classify extractive components. Hydrophilic extractives are the soluble molecules in high-polarity solvents, such as ethanol and water, while hydrophobic extractives are only soluble in low-polarity solvents, such as hexane and ether.

Softwood plants contain hydrophobic extractives or resins that can reach up to 15% of the total sample mass. Oleo-resins, which are composed of terpenes and fatty acids (free or esterified), are the most abundant. Hardwood samples, with

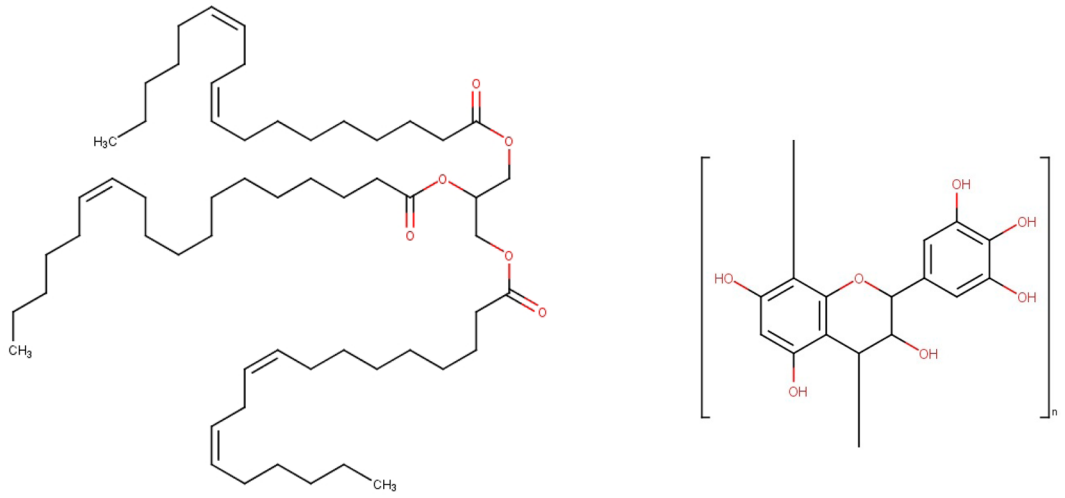

Figure 3. Reference species to represent hydrophobic and hydrophilic extractive components.

extractives (usually <2%), mostly contain wood-resin and are mainly constituted by fatty acids. Triglycerides, with a high presence of linoleic acid, are the most common hydrophobic extractives; these are found in many different plant sources. On this basis, we selected a new reference component (TGL: $C_{57}H_{100}O_7$), with a very high C and H content, to represent hydrophobic extractives.

Hydrophilic extractives are typically phenolic compounds with antioxidant properties, thereby serving a protective role in plants, and they are mainly present in the external organs (bark and leaves). They can be sorted into flavonoids and nonflavonoids, the second group being the most abundant and including phenolic acids and tannins. In particular, during the plant aging process, the condensed tannins are the result of flavonoids polymerization.

Condensed tannins contain complex chemical structures of polyphenolic compounds that have higher reactivity toward formaldehyde than phenol. Tannin species, because of their structure, are interesting in applications as adhesives and substitutes for phenol in phenol-formaldehyde resins. Most common commercial tannin species mainly come from the bark of mimosa, quebracho, pine, and eucalyptus.[27] In order to describe these phenolic species, we introduced a new lumped reference component (TANN, $C_{15}H_{12}O_7$), with a low H content, which is well-represented by a polymer of gallocatechin.

Figures 1 and 3 show the structures of the seven reference species considered here to describe the pyrolysis behavior of the different biomasses. Figure 4 shows how the new species, representative of extractives in terms of resin (TGL) and tannin (TANN) species, allows a significant extension of the characterization method. The procedure is the same reported for the previous model, based on the atomic H/C/O balances.

While the reference species RM-1 remains a proper average of cellulose and hemicellulose, the reference lignin mixtures (RM-2 and RM-3) become more flexible and they can move toward the reference species TGL or TANN, depending on the biomass composition, including, in this way, most of the biomass samples. Biomass samples contained in the shadowed area of Figure 2 are characterized by using the reference mixtures RM obtained with the default $\alpha/\beta/\gamma$ splitting

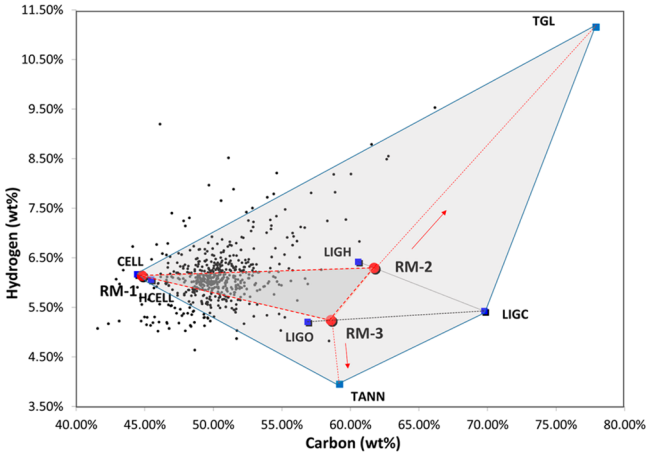

Figure 4. Extended biomass characterization. H% vs C% plot of biomass samples along with their reference species (daf basis).

parameters. As shown in Figure 4, for biomass rich in hydrogen, the amount of TGL progressively increases in the RM-2 mixtures. Similarly, for biomass with low hydrogen content, the reference mixture RM-3 increases its content of the reference component of tannin species (TANN).

As an example, the hybrid poplar[19] with an elemental composition (on a daf basis) of H/C/O = 0.0565/0.5092/0.4343, outside the applicability range of the previous model, is now characterized including 20% TANN in RM-3. Thus, the splitting parameters become $\alpha/\beta/\gamma/\delta/\varepsilon$ = 0.6/0.8/0.8/1/0.8, where the value ε = 0.8 means that 80% of lignins (LIGO and LIGC) and 20% of TANN are combined to define RM-3. In this way, the biomass with low H content also enters into the characterization region. The solution of the linear system of H/C/O balance equations gives the following mass composition of the reference mixtures:

RM-1 = 0.5597 RM-2 = 0.0020 RM-3 = 0.4384

The amount of the reference mixture RM-2 is very low, because of the low hydrogen content. Thus, these biomass results are mostly split between RM-1 and RM-3. From these

values and the splitting parameters, the following mass composition for the seven reference species is obtained:

CELL = 0.3627 HCELL = 0.1970
LIGH = 0.0017 LIGO = 0.3181 LIGC = 0.0489
TGL = 0.0000 TANN = 0.0716

Similarly, the olive husks[26] with H/C/O = 0.0696/0.5489/0.3815 are characterized by the following mass composition:

CELL = 0.3484 HCELL = 0.1892
LIGH = 0.2474 LIGO = 0.0170 LIGC = 0.0392
TGL = 0.1589 TANN = 0.0000

These values are obtained by using the splitting parameters: $\alpha/\beta/\gamma/\delta/\varepsilon$ = 0.6/0.8/0.8/0.8/1. The value δ = 0.8 means that 80% of lignins (LIGH and LIGC) and 20% of TGL are combined to obtain RM-2, and this condition allows this biomass with high H content to enter the characterization region.

While the default values of $\alpha/\beta/\gamma$ remain unchanged, the splitting parameters δ and ε are progressively reduced, increasing in this way the extractive content, in order to respect a feasible composition (i.e., non-negative values for all the seven reference components).

As a result of this extension, all the biomasses contained in the shadow area can be described as a linear combination of the seven reference components. In this way, the characterization procedure is able to process more than 90% of the lignocellulosic biomasses. Moreover, because of the limited amount of extractives, the characterization is only partially changed for the biomass samples previously described with only five original reference components.

The new biomass characterization method, with seven reference components, involves five degrees of freedom. It is then possible to select the three reference mixtures by properly changing not only the previous three splitting parameters (α, β, and γ) but also the relative content of tannin and triglyceride species in RM-2 and RM-3 mixtures (δ and ε). For this purpose, a nonlinear regression method[28,29] was applied in order to determine the optimal splitting parameters as a function of the H and C content of the biomass sample. Optimal parameters were obtained by minimizing the deviations between the predicted and experimental composi-tion, in terms of cellulose, hemicellulose, lignin, and extractives. Namely, three different sets of optimal splitting parameters are obtained by considering the entire set of biomasses (OPT1), the subset of wood samples (OPT2), and the grass/cereal samples (OPT3).

Details on this optimization process and obtained results are reported in the Supporting Information, but it is relevant to remark that the optimal splitting parameters are not very different from the previously suggested ones and (as discussed in Section 4) their effect on biomasss pyrolysis is very limited.

4.1. Parity Diagrams of Structural Components. In order to verify the reliability and the uncertainty of the characterization method, Figure 5 reports the parity diagrams of the calculated and experimental composition of the biomass reported in the Supporting Information whose structural composition was determined experimentally. To perform this analysis, both experimental and predicted values were organized into cellulose, hemicellulose, lignin, and extractives. For the model predictions, lignin represents the sum of LIGH, LIGC, and LIGO, while the extractives are the sum of TGL and TANN. The complete comparisons between model predictions and experimental data are reported in the Supporting Information. Figure 5 distinguishes the biomass families, in terms of hardwood, softwood, grass, and cereals. Relevant differences exist between the compositions of wood and grass/cereal samples. Namely, wood plants have higher cellulose/hemicellulose ratios, while extractives are more abundant in grass plants. Table 4 reports the corresponding average and standard deviations. The mean square deviations can be at least partially explained by considering, on one hand, the strong simplifications in the selection of reference species, but on the other hand, also the large variety of analytical methods for the determination of structural and biochemical composition, as well as the different uncertainties of the experimental information. It is also important to highlight that predicted extractives are the sum of two reference components, tannins and triglycerides, whose compositions are very different.

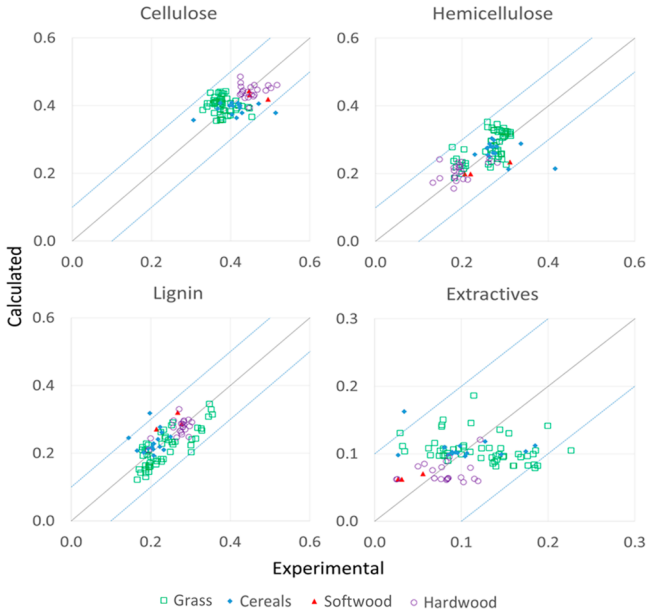

Figure 5. Parity diagrams of experimental and predicted biomass composition in terms of cellulose, hemicellulose, lignin, and extractives.

Table 4. Mean Square and Average Deviations of Cellulose, Hemicellulose, Lignins, and Extractives

	cellulose	hemicellulose	lignin	extractives
Extended Characterization (96 Biomass Samples)				
experimental average	0.4045	0.2521	0.2366	0.1068
calculated average	0.4101	0.2603	0.2322	0.0974
average deviation	−0.0057	−0.0087	0.0051	0.0093
mean square deviation	0.0017	0.0018	0.0014	0.0025
Previous Characterization, without Extractives (42 Biomass Samples)				
experimental average	0.4094	0.2466	0.2470	0.0969
calculated average	0.3691	0.2406	0.3902	0.
average deviation	0.0403	0.0060	−0.1432	0.0969
mean square deviation	0.0719	0.0572	0.1548	
Sheng and Azevedo Characterization[30] (73 Biomass Samples)				
experimental average	0.4031	0.2394	0.2567	0.1008
calculated average	0.3749	0.3587	0.2665	0.
average deviation	0.0329	−0.1188	−0.0155	0.1008
mean square deviation	0.0545	0.1448	0.0760	

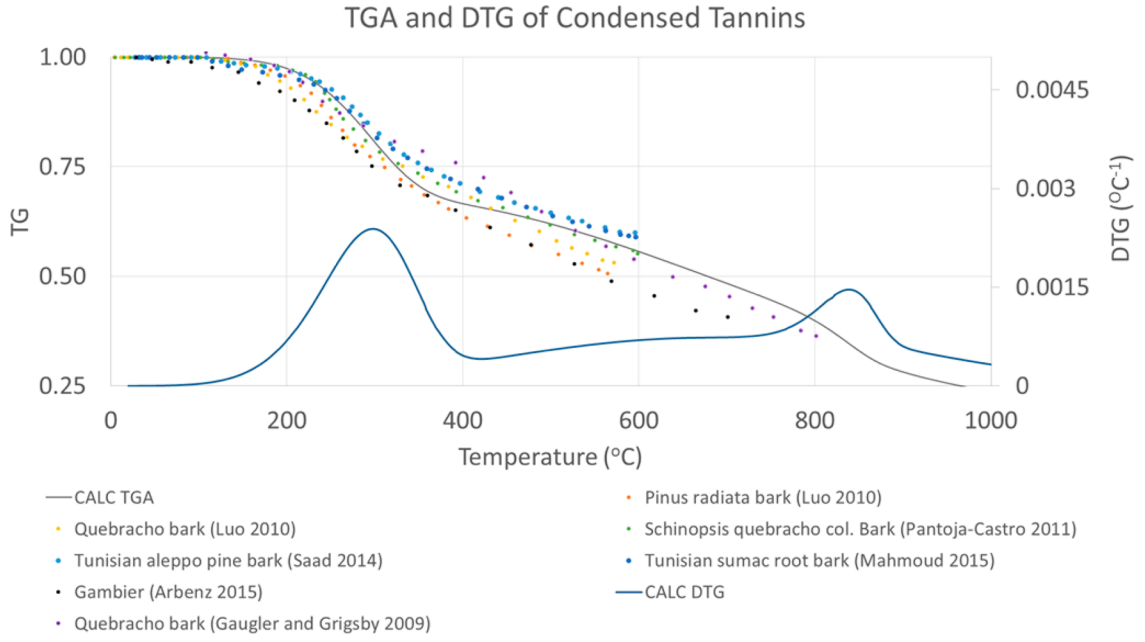

Figure 6. TGA and DTGA of condensed tannins samples heated at a rate of 10 K/min (model predictions (lines) and experimental data (symbols)).

Experimental data with a distinction between these two classes of components would be useful to improve the characterization method and to reduce the large scatter of extractives.

The average content of extractive species inside these biomass samples is ∼10%. Therefore, despite the persisting deviation, there is a clear improvement when the mean square deviations of predicted values are compared with the original and extended model. Only 42 biomass samples whose biochemical compositions are known can be characterized by the previous model (see Figure 1). In particular, there is a large overestimation (∼14%) of the lignins and an underestimation of ∼4% cellulose. This result is mainly due to the chemical similarity of LIGO and condensed tannins. Table 4 also compares these characterization methods with the method proposed by Sheng and Azevedo.[30] This characterization method was applied using the CPD model,[31] when biochemical composition was not available.[32] The mass fractions of cellulose and lignin are evaluated as a function of the ratios of oxygen and hydrogen to carbon (O/C and H/C, respectively) in biomass and the volatile matter (VM). Then, it is necessary to have both proximate and ultimate elemental analysis for each biomass. As a consequence, only 73 biomass samples are considered here. The analysis of Table 4 clearly highlights the great improvements of the proposed extended characterization method, when compared with the other two.

5. MULTISTEP KINETIC SCHEME OF BIOMASS PYROLYSIS

As already mentioned, biomass decomposition is treated as a linear combination of the pyrolysis products of the reference components: cellulose, hemicellulose, three lignins, and the two extractive components.[10] Each component decomposes independently through a multistep, branched mechanism of first-order, lumped reactions, producing intermediate solid species, char, gases, tars, and adsorbed gases. The revised kinetic mechanism of biomass pyrolysis (limited to the first five components) is reported in ref 24. The rate expressions and stoichiometries of these lumped reactions were originally derived from experimental information[10] and were upgraded continuously, based on new experimental data and comparisons across a wider range of experimental conditions.[33,34] In order to analyze the biomass pyrolysis with the extended characterization method, it is first necessary to define the solid-phase kinetics of the pyrolysis of the new reference species of extractive components, extending, in this way, the multistep kinetic scheme of biomass pyrolysis.

5.1. Condensed Tannins. The pyrolysis kinetics of the TANN reference species was mainly based on several literature works.[27,35−42] Galletti et al.[37] analyzed the pyrolysis of wine condensed tannin samples, observing relevant amounts of phenol and catechol species. Luo et al.[38] observed a two-step decomposition of condensed tannins, the first one at 250 °C and the second with relatively lower rates of weight loss, with residue weighing up to 40% at 700 °C.[42] Thermogravimetric analysis (TGA) of Tunisian sumac root bark tannins heated at 10 °C/min under nitrogen were studied by Mahmoud et al.[27] Similarly, Saad et al.[41] studied the TGA curves of Aleppo pine, mimosa, and quebracho tannins always heated at 10 °C/min under nitrogen. Apart from the removal of the residual water, they observed a first release of volatile species at temperatures between 125 °C and 300 °C, and a second degradation step, possibly coupled with relevant condensation and charification reactions. Figure 6 shows a comparison between model predictions and experimental data for some TGA of condensed tannins reported in the previous referred works.

In agreement with the experiments, the proposed mechanism is constituted by two reactions in series; it is reported in Table 5. The first is a fission of the heterocyclic ring, with a peak of mass loss at 280−310 °C, producing phenolic species and forming an intermediate lumped species (ITANN: $C_9H_6O_6$), which remains in the metaplastic or solid phase. Then, a successive lumped slow reaction occurs, releasing gases (by decarbonylation and dehydration) and producing solid species, by reticulation and charification processes (thus explaining the relatively high amount of solid residue).

5.2. Resins and Triglycerides. The kinetic mechanism of resins and triglycerides (TGL) is mainly based on experimental

Table 5. Lumped Reactions of Extractive Species (TANN and TGL)

reaction	A [s^{-1}]	activation energy [kcal/kmol]
TANN → FENOL + ITANN	50.	11 000
ITANN → 5CHAR + 3CO + $GCOH_2$ + $2H_2O$	0.015	6100
TGL → acrolein + 3FFA	7×10^{12}	45 700

works related to the TGA of soybean and corn oils, which are mixtures of triglycerides containing mostly unsaturated fatty acids.[43,44] Using the oil mixtures instead of a pure compound allows the kinetic model of the lumped species TGL to better behave as real biomasses. The pyrolysis of triglycerides releases acrolein (C_2H_3CHO), together with two fatty acids and one aldehyde.[45,46] By adding a water molecule to the lumped reference species TGL, it is possible to simplify the lumped kinetic model and TGL can release only acrolein and three free fatty acids (FFA, $C_{18}H_{32}O_2$). According to the experiments, the complete TGL devolatilization, without significant residue, is well-represented by single-step kinetics, as reported in Table 5.

Figure 7 reports a comparison between experimental data[43,44] and model predictions. With a heating rate of 10 K/min, at ∼350 °C acrolein is formed, together with FFA, which is a lumped species representing a mixture of FFAs. Successive secondary gas-phase reactions of FFA, here considered as a linoleic acid, are already considered in the overall kinetic scheme of gas-phase pyrolysis and oxidations of hydrocarbon and oxygenated fuels.[47,48]

6. RESULTS AND VALIDATION OF THE BIOMASS PYROLYSIS MODEL

The extended multistep kinetic scheme of biomass pyrolysis involves seven reference components, and it is reported in the Supporting Information. For biomass samples, whose composition was already described with the previous characterization method, the inclusion of extractive reference species does not modify the previous pyrolysis behavior. Figure 8 shows a couple of comparisons between the model predictions and the experiments for the pyrolysis of almond shell[49] and softwood bark.[25] The elemental composition and the predicted amount of reference species, characterized with and without extractives, are reported in Table 6. The elemental biomass compositions are also schematically reported in the inner C/H boxes of Figure 8, showing that both these biomasses are inside the triangle of Figure 2. The differences between the predictions of the previous and the extended model are very limited and well within the deviations, with respect to the experimental data. The DTG of the reference components are also reported, together with the TG of almond shell, in order to better highlight their thermal behavior.

Figure 9 shows a couple of comparisons between model predictions and experiments of pyrolysis of oil palm shell[50] and wheat straw.[51] Their elemental compositions are reported in Table 6, together with the predicted biochemical composition, including extractive species. As clearly shown in the inner C/H diagrams, these biomasses are outside the previous characterization region; therefore, the previous method cannot be applied. Again, the comparisons show reasonable agreement, even if some major deviations are observed for the initial decomposition of wheat straw.

6.1. Model Sensitivity to Characterization Parameters.

The extended characterization procedure involves five degrees of freedom (α, β, γ, δ, and ε). Figure 10 shows a parametric sensitivity analysis to these feedstock characterization parameters. Experimental TGA of switchgrass[51] is used to verify the effect of the different predicted compositions, obtained with different splitting parameters. As discussed in the Supporting Information, three different sets of optimal splitting parameters are obtained by considering the entire set of biomasses (OPT1), the subset of wood samples (OPT2), and the grass/cereal samples (OPT3). Table 6 shows the elemental composition (dry and ash free, daf) and the predicted biochemical composition, in terms of the relative amount of reference components with the three different sets of parameters. Predicted cellulose amounts range from 39% to 45%, 20%−29% for hemicellulose, 16%−25% for lignins, and, finally, 6%−8% for extractives. Despite these significant differences in the amount of reference components, the four predicted devolatilization behaviors remain very similar and agree reasonably well with the experimental data. Moreover, uniformity and similarity is also observed for the yields of released gas and tar species. This shows that the pyrolysis behavior is not very sensitive to the degrees of freedom chosen for the characterization procedure. It is also relevant to highlight that the proposed method is completely predictive,

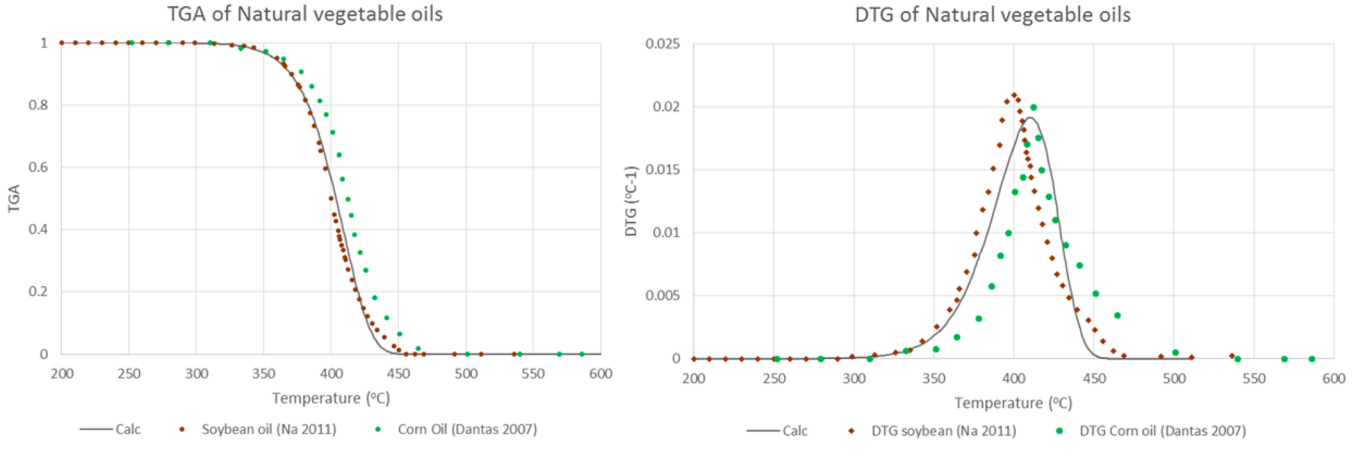

Figure 7. TGA and DTG of lumped species for resins (TGL) and natural vegetable oils, heated at 20 K/min (model predictions (lines) and experimental data (symbols)).

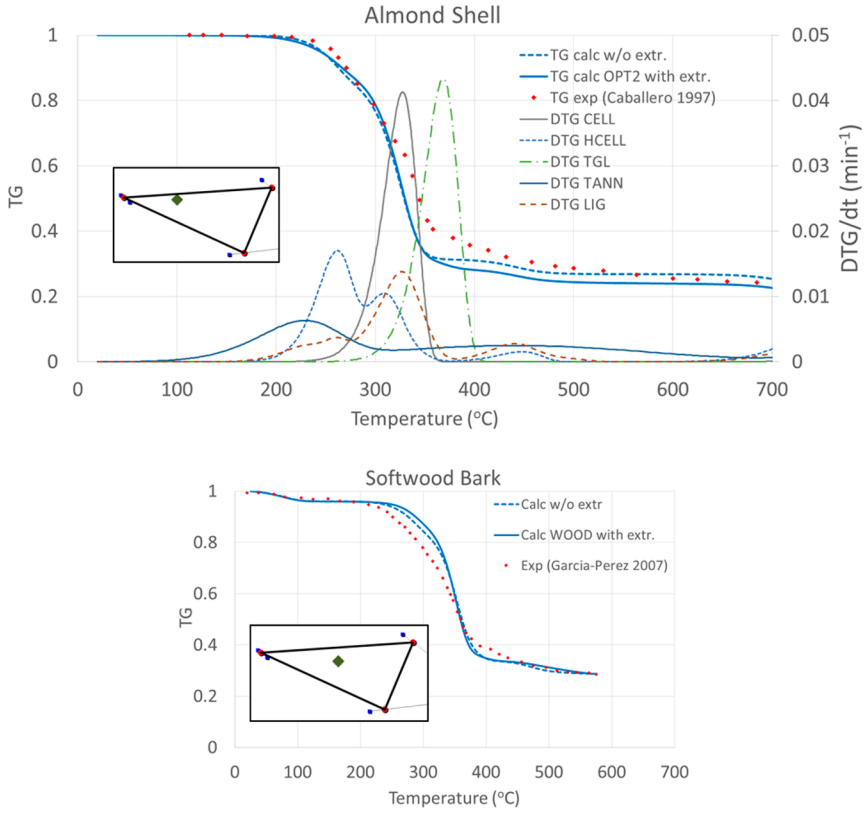

Figure 8. Pyrolysis of almond shell[49] (2 K/min) and softwood bark[25] (10 K/min). Comparisons between experimental data (points) and predictions of the extended (solid line) and the previous characterization model (dashed line) are shown.

Table 6. Elemental Composition (Dry and Ash-Free) and Predicted Biochemical Composition of Biomass Samples Used in Section 4

	Elemental Analysis (daf wt %)			Reference Components (Mass Fraction)								
characterization method	C	H	O	CELL	HCELL	LIGH	LIGO	LIGC	TGL	TANN	H_2O	ash
almond shell												
w/o extr.	0.509	0.061	0.430	0.384	0.25	0.225	0.076	0.064			0	0
with extr. OPT2	0.509	0.061	0.430	0.446	0.203	0.077	0.143	0.063	0.037	0.032	0	0
softwood bark												
w/o extr.	0.534	0.060	0.406	0.278	0.181	0.177	0.217	0.083			0.04	0.024
with extr. OPT2	0.534	0.060	0.406	0.398	0.171	0.077	0.000	0.219	0.022	0.049	0.04	0.024
oil palm shell												
with extr. OPT2	0.524	0.065	0.411	0.342	0.197	0.283	0.007	0.025	0.055	0.000	0.05	0.042
wheat straw												
with extr. OPT1	0.493	0.057	0.450	0.371	0.234	0.000	0.160	0.020	0.002	0.105	0.09	0.019
switchgrass												
w/o extr.	0.493	0.061	0.447	0.431	0.234	0.145	0.083	0.034			0.028	0.045
with extr. OPT3	0.493	0.061	0.447	0.450	0.203	0.048	0.168	0.000	0.032	0.026	0.028	0.045
with extr. OPT2	0.493	0.061	0.447	0.393	0.284	0.004	0.151	0.011	0.041	0.042	0.028	0.045
with extr. OPT1	0.493	0.061	0.447	0.388	0.287	0.059	0.100	0.034	0.059	0.001	0.028	0.045

simply requiring the ultimate analysis. Therefore, both the rough assumption on the biomass composition, in terms of a few reference components, and their lumped kinetics can justify the observed deviations.

Finally, it is important to emphasize that, while this extension of the multistep kinetic model of biomass pyrolysis allows the treatment and description of the thermal behavior of a very wide range of biomass samples, the kinetic model still is not able to properly account for ash catalytic effects. It is indeed well-known for several years that higher yields of bio-oil are obtained from the fast pyrolysis of biomass feeds with a low ash content.[52] Thus, the next step in the development of a more general kinetic model of biomass pyrolysis could consist of modifying the reaction scheme, or simply the kinetic parameters of specific reactions to account for this effect. An example of this attempt was recently proposed by Trendewicz et al.,[53] who studied the effect of potassium on the reaction kinetics of cellulose pyrolysis.

7. CONCLUSIONS

Taking advantage of the very large set of experimental data collected and reported in the Supporting Information, this work

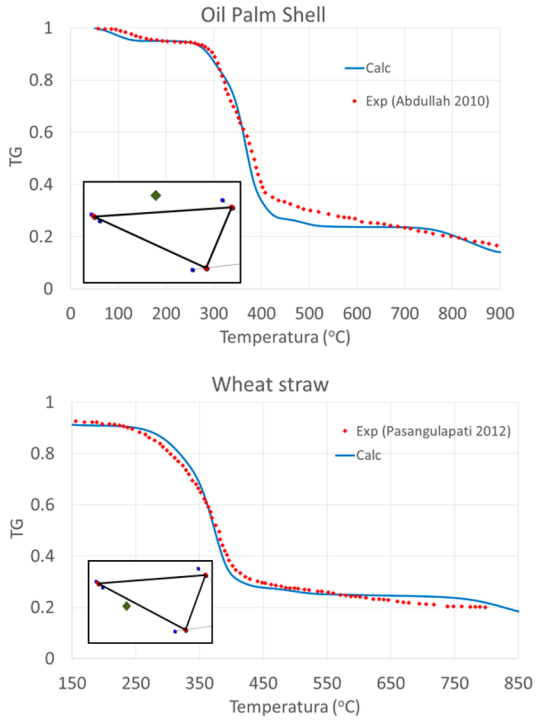

Figure 9. Pyrolysis of oil palm shell (20 K/min)[50] and wheat straw (80 K/min).[51] Elemental biomass composition is reported in the inner C/H box. Comparisons between experimental data (points) and extended model predictions (solid line).

extended the validity range of a biomass characterization method[10] by including a couple of extractive species, as new reference components. A lumped species representative of condensed tannins (hydrophilic extractive), together with a lumped resin or triglyceride (hydrophobic extractive), allowed a useful extension of the biomass characterization method, now able to describe most ligno-cellulosic biomasses. The corresponding multistep kinetic model of the biomass pyrolysis simply required the definition of the pyrolysis kinetics of the two new reference species.

For biomass samples contained in the range of the original characterization model, the new pyrolysis model is proven to be fully consistent with the previous one, already validated in a wide range of different conditions.[10,24,33,34] Several comparisons of pyrolysis of biomass samples, previously outside the applicability range of the characterization method, validate the proposed extension. Moreover, it is also shown that the model is not very sensitive to the splitting parameters applied in this biomass characterization approach. The method is completely predictive and only requires the ultimate analysis of the biomass sample.

Spreadhseet of data from the Creck Biomass Database (XLSX)
Estimation of optimal characterization parameters and multistep kinetics scheme (PDF)

AUTHOR INFORMATION

Corresponding Author

*Tel.: 39 02 2399 3250. E-mail: eliseo.ranzi@polimi.it.

Notes

The authors declare no competing financial interest.

ACKNOWLEDGMENTS

P.D. gratefully acknowledges the financial support from CAPES Foundation, Ministry of Education of Brazil—Science without Borders Mobility Program—Full PhD Scholarship Process No. 10131/13-2.

REFERENCES

(1) Heidenreich, S.; Foscolo, P. U. New concepts in biomass gasification. *Prog. Energy Combust. Sci.* **2015**, *46*, 72−95.
(2) Bridgwater, A. V. Review of fast pyrolysis of biomass and product upgrading. *Biomass Bioenergy* **2012**, *38*, 68−94.
(3) Ranzi, E.; Corbetta, M.; Manenti, F.; Pierucci, S. Kinetic modeling of the thermal degradation and combustion of biomass. *Chem. Eng. Sci.* **2014**, *110*, 2−12.
(4) Sfetsas, T.; Michailof, C.; Lappas, A.; Li, Q.; Kneale, B. Qualitative and quantitative analysis of pyrolysis oil by gas chromatography with flame ionization detection and comprehensive

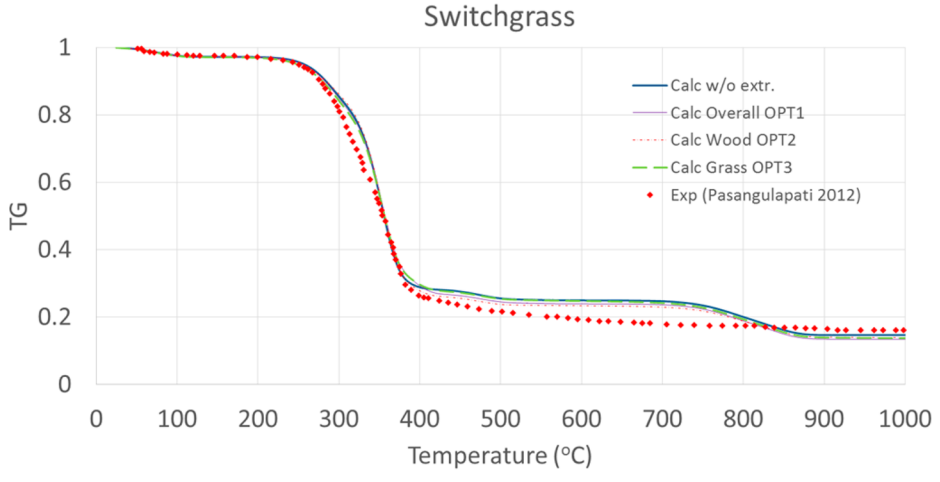

Figure 10. Pyrolysis of switchgrass at 10 K/min.[51] Comparisons between experimental data (points) and different model predictions (solid lines). Detailed compositions are given in Table 6.

two-dimensional gas chromatography with time-of-flight mass spectrometry. *J. Chromatogr. A* **2011**, *1218* (21), 3317−3325.
(5) Djokic, M. R.; Dijkmans, T.; Yildiz, G.; Prins, W.; Van Geem, K. M. Quantitative analysis of crude and stabilized bio-oils by comprehensive two-dimensional gas-chromatography. *J. Chromatogr. A* **2012**, *1257*, 131−140.
(6) Yildiz, G.; Pronk, M.; Djokic, M.; van Geem, K. M.; Ronsse, F.; Van Duren, R.; Prins, W. Validation of a new set-up for continuous catalytic fast pyrolysis of biomass coupled with vapour phase upgrading. *J. Anal. Appl. Pyrolysis* **2013**, *103*, 343−351.
(7) Weng, J.; Jia, L.; Wang, Y.; Sun, S.; Tang, X.; Zhou, Z.; Kohse-Höinghaus, K.; Qi, F. Pyrolysis study of poplar biomass by tunable synchrotron vacuum ultraviolet photoionization mass spectrometry. *Proc. Combust. Inst.* **2013**, *34* (2), 2347−2354.
(8) Miller, R.; Bellan, J. A generalized biomass pyrolysis model based on superimposed cellulose, hemicellulose and liqnin kinetics. *Combust. Sci. Technol.* **1997**, *126* (1−6), 97−137.
(9) Grønli, M. G.; Varhegyi, G.; Di Blasi, C. Thermogravimetric analysis and devolatilization kinetics of wood. *Ind. Eng. Chem. Res.* **2002**, *41* (17), 4201−4208.
(10) Ranzi, E.; Cuoci, A.; Faravelli, T.; Frassoldati, A.; Migliavacca, G.; Pierucci, S.; Sommariva, S. Chemical kinetics of biomass pyrolysis. *Energy Fuels* **2008**, *22* (6), 4292−4300.
(11) Blondeau, J.; Jeanmart, H. Biomass pyrolysis at high temperatures: Prediction of gaseous species yields from an anisotropic particle. *Biomass Bioenergy* **2012**, *41*, 107−121.
(12) Anca-Couce, A.; Mehrabian, R.; Scharler, R.; Obernberger, I. Kinetic scheme of biomass pyrolysis considering secondary charring reactions. *Energy Convers. Manage.* **2014**, *87*, 687−696.
(13) Grønli, M. G. *A theoretical and experimental study of the thermal degradation of biomass*; Dr.Ing./Ph.D. Thesis, Norwegian University of Science and Technology, Trondheim, Norway, 1996.
(14) Demirbas, A. Combustion characteristics of different biomass fuels. *Prog. Energy Combust. Sci.* **2004**, *30* (2), 219−230.
(15) Williams, A.; Jones, J.; Ma, L.; Pourkashanian, M. Pollutants from the combustion of solid biomass fuels. *Prog. Energy Combust. Sci.* **2012**, *38* (2), 113−137.
(16) Parikh, J.; Channiwala, S.; Ghosal, G. A correlation for calculating elemental composition from proximate analysis of biomass materials. *Fuel* **2007**, *86* (12), 1710−1719.
(17) Shen, J.; Zhu, S.; Liu, X.; Zhang, H.; Tan, J. The prediction of elemental composition of biomass based on proximate analysis. *Energy Convers. Manage.* **2010**, *51* (5), 983−987.
(18) Sluiter, J. B.; Ruiz, R. O.; Scarlata, C. J.; Sluiter, A. D.; Templeton, D. W. Compositional analysis of lignocellulosic feedstocks. 1. Review and description of methods. *J. Agric. Food Chem.* **2010**, *58* (16), 9043−9053.
(19) National Renewable Energy Laboratory (NREL). *Biomass Feedstock Composition and Property Database*, 2015.
(20) International Energy Agency (IEA). *Bioenergy Task 32—BioBank*, 2015.
(21) Energy Research Centre of the Netherlands (ECN). *Phyllis2—Database for Biomass and Waste*, 2015.
(22) Reisinger, K.; Haslinger, C.; Herger, M.; Hofbauer, H. (BIOBIB). *BIOBIB—A Database for Biofuels*, 1996.
(23) Faravelli, T.; Frassoldati, A.; Migliavacca, G.; Ranzi, E. Detailed kinetic modeling of the thermal degradation of lignins. *Biomass Bioenergy* **2010**, *34* (3), 290−301.
(24) Corbetta, M.; Frassoldati, A.; Bennadji, H.; Smith, K.; Serapiglia, M. J.; Gauthier, G.; Melkior, T.; Ranzi, E.; Fisher, E. M. Pyrolysis of centimeter-scale woody biomass particles: Kinetic modeling and experimental validation. *Energy Fuels* **2014**, *28* (6), 3884−3898.
(25) Garcia-Perez, M.; Chaala, A.; Pakdel, H.; Kretschmer, D.; Roy, C. Vacuum pyrolysis of softwood and hardwood biomass: Comparison between product yields and bio-oil properties. *J. Anal. Appl. Pyrolysis* **2007**, *78* (1), 104−116.
(26) Demirbaş, A. Fuel characteristics of olive husk and walnut, hazelnut, sunflower, and almond shells. *Energy Sources* **2002**, *24* (3), 215−221.
(27) Ben Mahmoud, S.; Saad, H.; Charrier, B.; Pizzi, A.; Rode, K.; Ayed, N.; Charrier-El Bouhtoury, F. Characterization of sumac (*Rhus tripartitum*) root barks tannin for a potential use in wood adhesives formulation. *Wood Sci. Technol.* **2015**, *49* (1), 205−221.
(28) Buzzi-Ferraris, G.; Manenti, F. Outlier detection in large data sets. *Comput. Chem. Eng.* **2011**, *35* (2), 388−390.
(29) Buzzi-Ferraris, G.; Manenti, F. BzzMath: Library overview and recent advances in numerical methods. *Comput.-Aided Chem. Eng.* **2012**, *30* (2), 1312−1316.
(30) Sheng, C.; Azevedo, J. Modeling biomass devolatilization using the chemical percolation devolatilization model for the main components. *Proc. Combust. Inst.* **2002**, *29* (1), 407−414.
(31) Fletcher, T. H.; Kerstein, A. R.; Pugmire, R. J.; Solum, M. S.; Grant, D. M. Chemical percolation model for devolatilization. 3. Direct use of carbon-13 NMR data to predict effects of coal type. *Energy & Fuels* **1992**, *6* (4), 414−431.
(32) Vizzini, G.; Bardi, A.; Biagini, E.; Falcitelli, M.; Tognotti, L. *Prediction Of Rapid Biomass Devolatilization Yields with an Upgraded Version of the Bio-CPD Model*. Combustion Institute, Italian section: Torino, Italy, 2008.
(33) Dupont, C.; Chen, L.; Cances, J.; Commandre, J.-M.; Cuoci, A.; Pierucci, S.; Ranzi, E. Biomass pyrolysis: Kinetic modelling and experimental validation under high temperature and flash heating rate conditions. *J. Anal. Appl. Pyrolysis* **2009**, *85* (1), 260−267.
(34) Calonaci, M.; Grana, R.; Barker Hemings, E.; Bozzano, G.; Dente, M.; Ranzi, E. Comprehensive kinetic modeling study of bio-oil formation from fast pyrolysis of biomass. *Energy Fuels* **2010**, *24* (10), 5727−5734.
(35) Arbenz, A.; Avérous, L. Oxyalkylation of gambier tannin—Synthesis and characterization of ensuing biobased polyols. *Ind. Crops Prod.* **2015**, *67*, 295−304.
(36) Galletti, G. C.; Reeves, J. B. Pyrolysis/gas chromatography/ion−trap detection of polyphenols (vegetable tannins): Preliminary results. *Org. Mass Spectrom.* **1992**, *27* (3), 226−230.
(37) Galletti, G. C.; Modafferi, V.; Poiana, M.; Bocchini, P. Analytical pyrolysis and thermally assisted hydrolysis−methylation of wine tannin. *J. Agric. Food Chem.* **1995**, *43* (7), 1859−1863.
(38) Luo, C.; Grigsby, W.; Edmonds, N.; Easteal, A.; Al-Hakkak, J. Synthesis, characterization, and thermal behaviors of tannin stearates prepared from quebracho and pine bark extracts. *J. Appl. Polym. Sci.* **2010**, *117* (1), 352−360.
(39) Pantoja-Castro, M. A.; González-Rodríguez, H. Study by infrared spectroscopy and thermogravimetric analysis of tannins and tannic acid. *Rev. Latinoam. Quím.* **2011**, *39* (3), 107−112.
(40) Benyahya, S.; Aouf, C.; Caillol, S.; Boutevin, B.; Pascault, J. P.; Fulcrand, H. Functionalized green tea tannins as phenolic prepolymers for bio-based epoxy resins. *Ind. Crops Prod.* **2014**, *53*, 296−307.
(41) Saad, H.; Khoukh, A.; Ayed, N.; Charrier, B.; Charrier-El Bouhtoury, F. Characterization of Tunisian Aleppo pine tannins for a potential use in wood adhesive formulation. *Ind. Crops Prod.* **2014**, *61*, 517−525.
(42) Gaugler, M.; Grigsby, W. J. Thermal degradation of condensed tannins from radiata pine bark. *J. Wood Chem. Technol.* **2009**, *29* (4), 305−321.
(43) Na, J.-G.; Lee, H. S.; Oh, Y.-K.; Park, J.-Y.; Ko, C. H.; Lee, S.-H.; Yi, K. B.; Chung, S. H.; Jeon, S. G. Rapid estimation of triacylglycerol content of *Chlorella sp*. by thermogravimetric analysis. *Biotechnol. Lett.* **2011**, *33* (5), 957−960.
(44) Dantas, M. B.; Conceição, M. M.; Fernandes, V. J., Jr; Santos, N. A.; Rosenhaim, R.; Marques, A. L. B.; Santos, I. M. G.; Souza, A. G. Thermal and kinetic study of corn biodiesel obtained by the methanol and ethanol routes. *J. Therm. Anal. Calorim.* **2007**, *87* (3), 835−839.
(45) Meier, H.; Wiggers, V.; Zonta, G.; Scharf, D.; Simionatto, E.; Ender, L. A kinetic model for thermal cracking of waste cooking oil based on chemical lumps. *Fuel* **2015**, *144*, 50−59.
(46) Moldoveanu, S. C. *Pyrolysis of organic molecules: Applications to health and environmental issues*; Elsevier: Amsterdam, 2009.

(47) Saggese, C.; Frassoldati, A.; Cuoci, A.; Faravelli, T.; Ranzi, E. A lumped approach to the kinetic modeling of pyrolysis and combustion of biodiesel fuels. *Proc. Combust. Inst.* **2013**, *34* (1), 427−434.
(48) Ranzi, E.; Frassoldati, A.; Grana, R.; Cuoci, A.; Faravelli, T.; Kelley, A.; Law, C. Hierarchical and comparative kinetic modeling of laminar flame speeds of hydrocarbon and oxygenated fuels. *Prog. Energy Combust. Sci.* **2012**, *38* (4), 468−501.
(49) Caballero, J.; Conesa, J.; Font, R.; Marcilla, A. Pyrolysis kinetics of almond shells and olive stones considering their organic fractions. *J. Anal. Appl. Pyrolysis* **1997**, *42* (2), 159−175.
(50) Abdullah, S. S.; Suzana, Y.; Ahmad, M.; Ramli, A.; Ismail, L. Thermogravimetry study on pyrolysis of various lignocellulosic biomass for potential hydrogen production. *Int. J. Chem. Biol. Eng.* **2010**, *3* (3), 137−141.
(51) Pasangulapati, V. *Devolatilization characteristics of cellulose, hemicellulose, lignin and the selected biomass during thermochemical gasification: experiment and modeling studies*; Thesis, Oklahoma State University, Stillwater, OK, 2012.
(52) Raveendran, K.; Ganesh, A.; Khilar, K. C. Influence of mineral matter on biomass pyrolysis characteristics. *Fuel* **1995**, *74* (12), 1812−1822.
(53) Trendewicz, A.; Evans, R.; Dutta, A.; Sykes, R.; Carpenter, D.; Braun, R. Evaluating the effect of potassium on cellulose pyrolysis reaction kinetics. *Biomass Bioenergy* **2015**, *74*, 15−25.